The Detection of Low-Intensity Beams at the Holifield Radioactive Ion Beam Facility (HRIBF)

D. Shapira

*Physics Division, Oak Ridge National Laboratory**

T. A. Lewis

Engineering Science and Technology Division, Oak Ridge National Laboratory

Abstract. Beam diagnostic devices suitable for radioactive beam detection developed and implemented at HRIBF are described. These detectors are suited to measure low-intensity beams and can be used for tuning beams with intensities ranging from a few counts/sec to a few million particles/sec. The detectors can be used with heavy-ion beams at energies ranging from several keV*A to several MeV*A. The performance of these detectors, as well as future enhancement, will be presented. A variety of these detectors combined in different configurations have bean used at HRIBF for applications including beam profiling, beam timing, beam counting, and tagging isobars in the beam.

INTRODUCTION

Several factors make the delivery of, and experiments with, radioactive ion beams challenging. Among these are lower than customary beam intensities, admixture of other beam species and the residual activity generated by beam deposits. This presentation highlights some of the methods employed to meet these challenges at HRIBF.

BEAM DELIVERY

Initial beam tune

The main problem in tuning radioactive beams, especially during initial application, is their very low intensity. A sensitive phosphor should work if the beam's local density is sufficiently high, typically a few times 10^4/s focused to a few mm size spot. During initial stages of tuning one would need a "beam sniffer," i.e., a device that will indicate even the smallest amount of beam. *An* electronic particle detector would do if it also had the following properties:

- It can count at high rates (up to ~1MHz)
- Will not be prone to damage by heavy-ion bombardment.
- Avoid beam deposits on the detector or parts nearby.
- Provide position information (shape and size of beam).

The low-intensity beam diagnostic devices employed at the HRIBF facility fulfill at least part of the above criteria. **All** the devices are based on the detection of secondary emissions, from a surface hit by the beam (mostly electrons) with the detector of choice being a Micro-Channel-Plate (MCP). These detectors are fast and have very good efficiency for the heavy ions at the energies they are accelerated to at HRIBF [1,2,3,4].

TANDEMACCELERATOR

The locations of low-intensity beam diagnostic devices that were placed inside the tandem accelerator are shown in Figure 1. The device itself and characteristic performance curves (plate bias voltage vs counts) are shown in Figure 2. Note that we used a plate made of tantalum metal to stop the beam and that the electron current is amplified using a channeltron. This device is inserted into the beam path for brief periods in order to find the beam and is subsequently

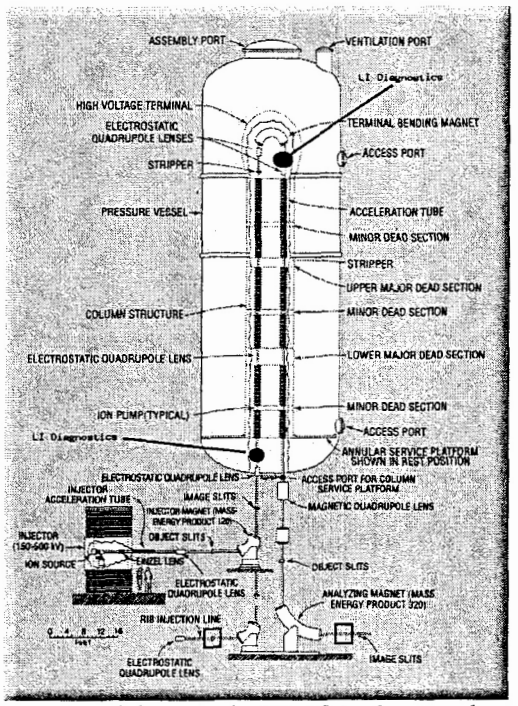

Figure 1. Schematic layout of tandem accelerator showing the location of the two low-intensity diagnostics modules (blue circles) inserted in the tandem column. The red squares show position of LI diagnostics at the entrance and exit to the accelerator.

withdrawn. Note that applying positive voltage to the plate causes a sudden drop in detected electron counting rate. The reasons for that drop are not fully understood, but it may be due to a combination of a decrease in channeltron efficiency for lower energy electrons and defocusing of the electrons by the retarding voltage. At any rate, this sudden drop in efficiency when measured can be used to extend the maximum detectable rate in single counting mode to more than 10^7 p/sec at which point the device can be replaced by charge integration readout (i.e., a faradav cup).

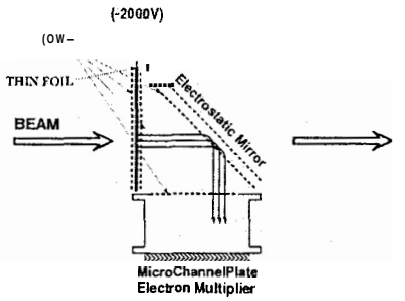

Figure 3. A beam-counting and timing detector. The electrons released during beam impact on the foil are accelerated and then redirected toward an MCP.

BEAM LINES

Similar beam counting devices, placed in beam lines outside the accelerator, are shown in Figure 3. These detectors are suitable for "beam sniffing," but can also serve as "pass through" timing detectors and can be used in experiments (e.g., as fast triggers). Secondary electrons are generated by beam particles hitting a thin (typically $10\,\mu g/cm^2$) carbon foil. The secondary electrons are accelerated and reflected on a grid toward an MCP. The ions continue almost unabated. The experimental setup used to check this detectors' timing resolution is shown in Figure 4. Spread in timing due to beam velocity variation is kept to a minimum by maintaining a short flight distance. Timing resolution clocked with 5.8 MeV α particles is about 140 ps (FWHM) for both detectors combined. The same test with 110 MeV ^{32}S beam yields 120ps time resolution and is shown in Figure 5. These detectors perform well at rates up to 10^6/s as is evident in Figure 6. The accelerating and reflecting grids are made with fine (0.2 μ) wires allowing for better then

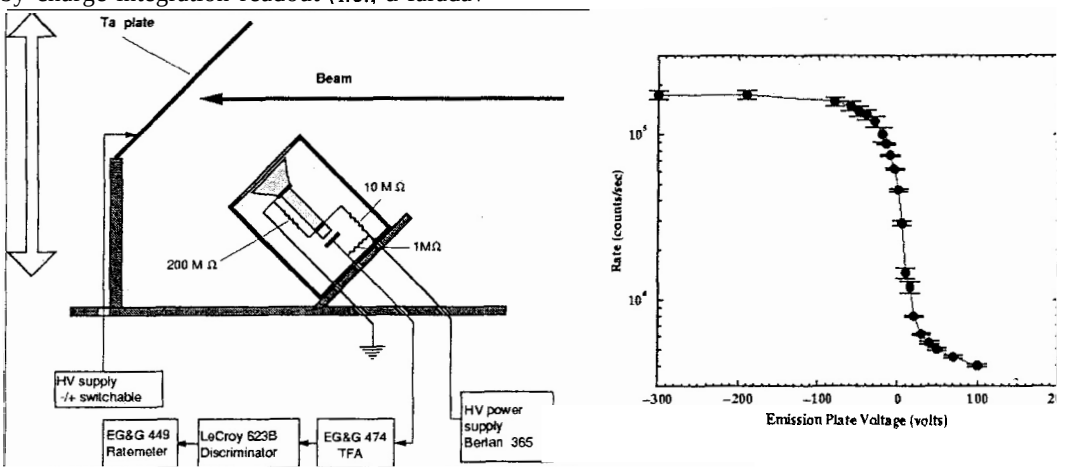

(a) (b)

Figure 2. A diagram of the LI beam diagnostic module operating inside the tandem. The device is used only to supply the count of beam particles and is withdrawn when beam intensity is raised.

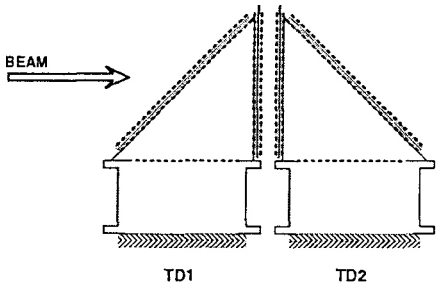

Figure 4. The setup used for testing the timing detectors. The detectors stacked so as to keep the flight path between the two foils to a minimum.

99.9% transmission.

BEAM VIEWING

A position-sensitive detector based on the detection of secondary electron emission is shown in Figure 7. Position sensing is accomplished by employing a MCP detector with a resistive layer anode. Unlike similar detectors, this device does not required rapid acceleration of electrons. There are no acceleration grids in the device and the foil is moderately biased (less the 1000V). Electrons are guided from the site of beam incidence on the foil to the MCP by means of a combination of electric and magnetic fields. This detector is fast and provides very accurate position information and is described in more detail elsewhere (see section E12 this conference and Ref. *5)*. This type of detector has been applied in several experiments as

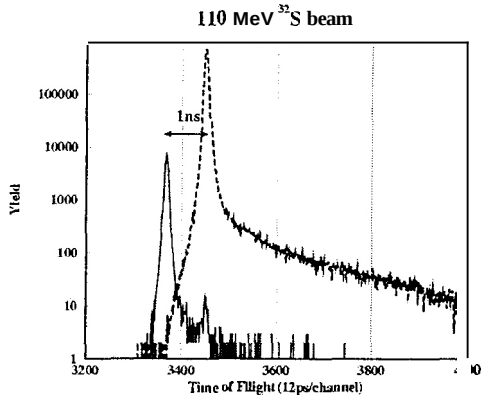

Figure 5. Time resolution and shape of the TOF spectrum for 120 MeV ^{32}S beam taken with the setup shown in Figure 4. Yield from a second exposure with an extra 1 ns decay and with 1% of the total count is also shown.

a low mass detector that yields accurate position and timing information [6,7]. In order to render the device more useful for beam tuning purposes, a semi-live display of beam particle positions acquired with this detector is used to emulate a phosphor screen [8]. **A** circular buffer (of size 2N) stores the XY-position coordinates from the most recent hits and is continuously updated. The last recorded position is added to the buffer and the oldest one in the buffer is eliminated. This buffer is displayed at a rep-rate that determines the phosphor's "decay time". Figure 8 provides two still snapshots of the display provided to the operator. It includes the "scintillating" phosphor display and bar graphs that continuously update the rate readout of three designated detectors.

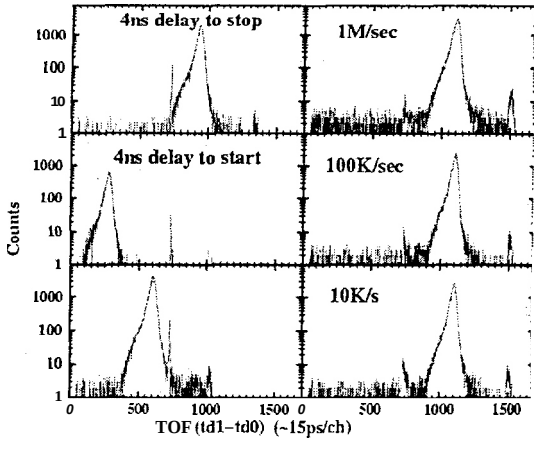

Figure 6. Time-of-flight spectrum for 240 MeV ^{58}Ni acquired with two detectors spaced about 1.2 m apart. The same spectrum taken at different beam rates is shown. There is a rise in random count, but the spectra look usable with all beam rates.

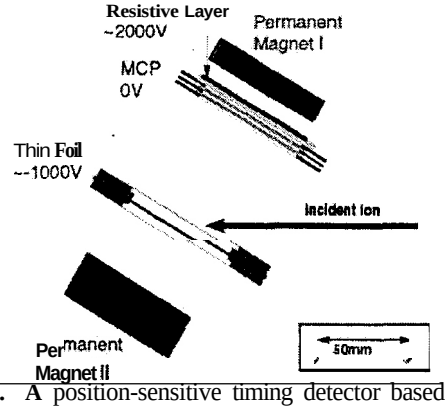

Figure 7. **A** position-sensitive timing detector based on detection of secondary electron emission. The detector uses the combination of magnetic and electric fields to transport electrons from the beam incidence site at the foil to the front of the MCP. The ratio of magnetic-field strength at the foil to that at the front of the MCP determines image magnification. The strength of the magnetic field near the foil determines image resolution.

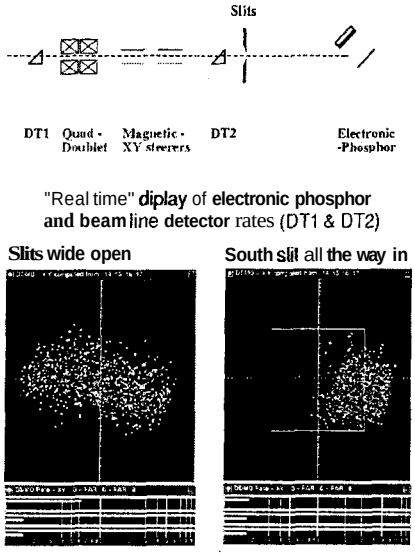

Figure **8.** Snapshots of the electronic phosphor display.

MONITORING BEAM PURITY

The nuclear reactions employed in the production of radioactive beam species are not very selective. **As** a result, isobars that tend to be close in mass to the selected beam product accompany the beam. Sometimes special chemistry enhances one species' delivery, but often the experimenter receives a "cocktail" of isobars. An example is accelerated ^{56}Ni beam. The **A** = 56 beam delivered will be mostly ^{56}Co. To separate these isobars would require 1/20000 mass resolution or, if we could detect nuclear charge, only 1/28 resolving power. Suppose we want to study evaporation residues and complex fragment yields following collisions of ^{56}Ni beam with ^{58}Ni and ^{40}Ca

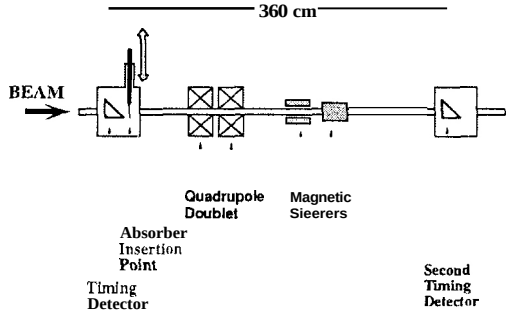

Figure **9.** The beamline components used in a test of the isobar separation technique. The absorber, which is a specially designed gas cell filled with isobutane, is inserted close to the first timing detector. Residual energy, rather then energy loss is measured via time-of-flight technique. This allows for the use of this technique for isobar tagging at a rate near 10^6/s.

targets that combine to form proton-rich compound nuclei. The physics is interesting, but there is a problem, there is no way to determine if the detected residue was produced from a nucleus formed by combining the target with ^{56}Ni or with ^{56}Co in the beam, unless we are able to tag ^{56}Ni nuclei before they interact. Energy loss depends on nuclear charge and, therefore, its measure is a good way to tag isobars. The experimental setup we used is shown in Figure 9. The salient features of this setup are the thin and fast timing detectors and the use of a specially constructed gas cell that provides an exceptionally uniform energy degrader/absorber. Repeated attempts to use thin foils as beam energy degraders proved fruitless, mainly due to > 3% non-uniformity. The degree of separation of ^{56}Co from ^{56}Ni that is achievable with this setup shown in Figure 10. The spectrum was simulated taking into account the timing resolution, anisochronism in beam trajectory, charge-state variation and energy straggling and shows adequate separation of the two isobars. These timing detectors can sample TOF data at rates of 10^6/s (see Figure 6). Note, however, that recorded data rates will depend on the rate of events of interest in the reaction. When an event of interest (detected

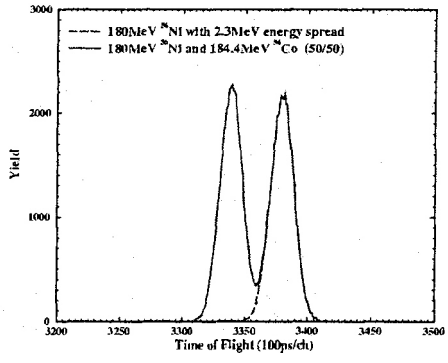

Figure 10. The anticipated separation of A = 56 isobars. Based on detail simulations.

evaporation residue or complex fragment) is produced in the reaction, the beam timing associated with this event is recorded and used to provide information on the precise energy of the particle entering the interaction and its identity (^{56}Ni or ^{56}Co). ^{56}Ni has not yet been delivered at HRIBF, but we did try this technique with a far more stringent test – separation of A = 132 isobars. Figure 11 shows, side by side, the simulated (predicted) separation achievable and the actual data taken for several mixtures of ^{132}Te/^{132}Sb/^{132}Sn. Further details and discussion of this technique are provided in Ref. 9.

FUTURE DEVELOPMENTS

Improved performance and reliability will be pursued continuously for all the devices listed above.

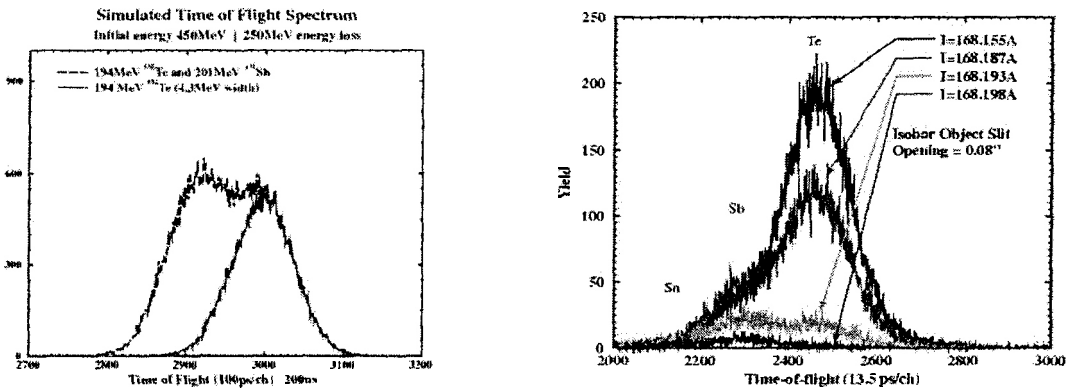

(a) (b)

Figure 11. Predicted tine-of-flight spectra for two A=132 isobars (a). The simulation for finite object size includes effect of detector timing resolution, anisochronous particle trajectories in the beamline, charge-state distribution, and straggling of the ions after the absorber Part (b) shows the data taken with **A** = 132 isobars accelerated at HRIBF to 450 MeV.

These include, but are not limited to, increasing available detector aperture and speed. We also plan to concentrate on a different problem, unique to radioactive beam facilities – monitoring the so-called "driver beams". These are high intensity beams used in the production of radioactive species, be it via fission, spallation, or fragmentation processes. Experience at HRIBF has shown that monitoring the driver beam's position and direction is important. **A** device, often used to monitor intense stored beams, is a Residual Gas Beam Profile Monitor (RGBPM) [Refs. 10,11,12]. The device detects ions produced by the interaction of beam particles with the residual gas atoms remaining in the evacuated beam pipe. The operating principle of such a device, as improved by us [13] to provide true **3-D** images of the beam trajectory, is illustrated in Figure 12.

The probability of ionizing a residual gas atom depends on the density of residual gas and the beam intensity **and** will produce well below one million ion-electron pairs at beam intensities exceeding 10^{14}/s and a residual gas pressure of 10^{-8} Torr thus providing a good and immediate sampling of the beam position. Following tests for radiation hardness of the different components, we plan to insert such a device in the beamline leading from the cyclotron to the ISOL production target.

REFERENCES

1. G. Gabor et al., Nucl. Instrum. Methods **130** (1975) 65.
2. W. Starzecki et al., Nucl. Instrum. Methods **193** (1982) 499.
3. Y. Zhang et al., Nucl. Instrum. Methods **B149** (1999) 477.
4. **D.** Shapira et al., Nucl. Instrum. Methods **A449** (2000) 396.
5. **D.** Shapira et al., Nucl. Instrum. Methods **A454** (2000) 409.
6. W. Krolas et al., Phys. Rev. C65 (2002) **031003(R).**
7. C. Barton et al., submitted to Phys. Lett..
8. W.T. Milner DDMAN, HRIBF Data acquisition computer manual.
9. **D.** Shapira et al., Nucl. Instrum. Methods **A490** (2002) 159.
10. J. Krider et al., Nucl. Instrum. Methods **A278** (1989) 660.
11. B. Hochadel et al., Nucl. Instrum. Methods **A343** (1994) 401.
12. T. Quinteros et al., Nucl. Instrum. Methods **A378** (1996) 35.
13. D. Shapira et al., Nucl. Instrum. Methods **A400** (1997) 185.

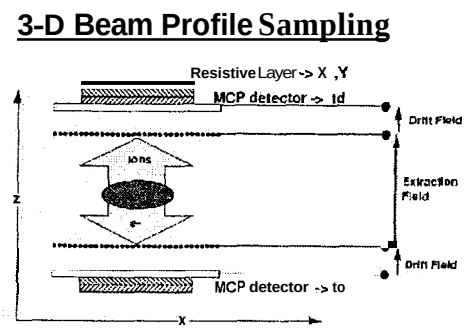

Figure 12. Principles of operation of a residual gas beam profile monitor that provides true 3-D samples of the beam profile.